

# Finite size scaling study of lattice models in the three-dimensional Ising universality class

Martin Hasenbusch\*

*Institut für Physik, Humboldt-Universität zu Berlin, Newtonstr. 15, 12489 Berlin, Germany*

(Received 11 May 2010; revised manuscript received 28 October 2010; published 23 November 2010)

We study the spin-1/2 Ising model and the Blume-Capel model at various values of the parameter  $D$  on the simple cubic lattice. To this end we perform Monte Carlo simulations using a hybrid of the local Metropolis, the single cluster and the wall cluster algorithm. Using finite size scaling we determine the value  $D^* = 0.656(20)$  of the parameter  $D$ , where leading corrections to scaling vanish. We find  $\omega = 0.832(6)$  for the exponent of leading corrections to scaling. In order to compute accurate estimates of critical exponents, we construct improved observables that have a small amplitude of the leading correction for any model. Analyzing data obtained for  $D = 0.641$  and  $0.655$  on lattices of a linear size up to  $L = 360$  we obtain  $\nu = 0.63002(10)$  and  $\eta = 0.03627(10)$ . We compare our results with those obtained from previous Monte Carlo simulations and high-temperature series expansions of lattice models, by using field-theoretic methods and experiments.

DOI: [10.1103/PhysRevB.82.174433](https://doi.org/10.1103/PhysRevB.82.174433)

PACS number(s): 05.50.+q, 05.70.Jk, 64.60.F-

## I. INTRODUCTION

In the neighborhood of a second-order phase transition various quantities diverge. For example, the correlation length, which characterizes the decay of the two-point correlation function, behaves as

$$\xi = f_{\pm} |t|^{-\nu} (1 + b_{\pm} |t|^{\theta} + ct + d_{\pm} |t|^{\theta'} + e_{\pm} |t|^{2\theta} + \dots), \quad (1)$$

where  $t = (T - T_c)/T_c$  is the reduced temperature,  $f_+$  and  $f_-$  are the amplitudes in the high- and the low-temperature phase, respectively, and  $\nu$  is the critical exponent of the correlation length. These power laws are affected by confluent corrections, such as  $b_{\pm} |t|^{\theta}$ ,  $d_{\pm} |t|^{\theta'}$ ,  $e_{\pm} |t|^{2\theta}$ , and nonconfluent ones such as  $ct$ . Critical exponents such as  $\nu$  and ratios of amplitudes such as  $f_+/f_-$  are universal. This means that they assume exactly the same value for any system within a given universality class. Also correction exponents such as  $\theta = \omega\nu \approx 0.5$  and ratios of correction amplitudes as  $b_+/b_-$  are universal. A universality class is characterized by the dimension of the system, the range of the interaction and the symmetry of the order parameter. For reviews on critical phenomena and the renormalization group (RG) see, e.g., Refs. 1–4. The critical exponents  $\alpha$  of the specific heat,  $\gamma$  of the magnetic susceptibility,  $\eta$  of the two-point correlation function at the critical point,  $\nu$  of the correlation length,  $\delta$  of the magnetization at the critical temperature as a function of the external field, and  $\beta$  of the spontaneous magnetization at a vanishing external field are related by so called scaling and hyperscaling relations. This allows to deduce all of them from two independent exponents.

Here we are concerned with three dimensions, short-range interactions, and a  $\mathbb{Z}_2$  symmetry of the order parameter. The best known model undergoing a phase transition in this universality class is the spin-1/2 Ising model in three dimensions with nearest neighbor interactions. Therefore this universality class is called the three-dimensional Ising universality class. This universality class is supposed to be realized in a huge range of experimental systems: binary mixtures, uniaxial magnets, or micellar systems, see, e.g., Refs. 4–6. Typically the estimates of critical exponents extracted from experimental data are less accurate than those

obtained by using the theoretical methods discussed below. For example, recent experimental estimates obtained from turbidity data for a methanol-cyclohexane mixture are  $\nu = 0.632(2)$  and  $\eta = 0.041(5)$ .<sup>7</sup>

Critical exponents and amplitude ratios have been computed by various theoretical methods such as field-theoretic methods or high-temperature (HT) series expansions and Monte Carlo (MC) simulations of lattice models. First let us briefly discuss results obtained by the  $\epsilon$  expansion,<sup>8</sup> where the dimension  $d$  of the system is given by  $d = 4 - \epsilon$  and the perturbative expansion in  $d = 3$ .<sup>9</sup> The  $\epsilon$  expansion of critical exponents has been computed up to  $O(\epsilon^5)$  (Ref. 10) while the perturbative expansion in  $d = 3$  has been computed up to seven loops<sup>11</sup> for the Ising universality class. Since both expansions are divergent, some kind of resummation is needed to extract numerical results for critical exponents. In the case of the  $\epsilon$  expansion the estimates reported in the literature are consistent among each other. As a representative result we report in Table I the one of Ref. 12. In Table I we also give results obtained from the perturbative expansion in  $d = 3$  using different resummation techniques. For a more complete compilation see, e.g., Ref. 4. In Table I we give the exponents  $\nu$ ,  $\eta$ , and the correction exponent  $\omega$ , since these are directly computed by using field-theoretic methods. In addition, we report the value of  $\gamma$  that can be compared with the results of the high-temperature series expansions reported below. Typically, the errors reported for the critical exponents obtained from the perturbative expansion in  $d = 3$  are smaller than those obtained from the  $\epsilon$  expansion. While the estimates for  $\nu$  are all consistent within the quoted errors, clear variations can be observed for  $\eta$ ,  $\gamma$ , and  $\omega$ . For a discussion of the different resummation schemes that have been used, we refer the reader to Ref. 16.

In Table II we summarize recent results obtained from lattice models. For an exhaustive summary of previous works see Ref. 4. The authors of Ref. 17 have analyzed the high-temperature series expansion of improved models on the simple cubic lattice up to  $O(\beta^{25})$ , where  $\beta = 1/k_B T$  is the inverse temperature. One of these models is studied here using Monte Carlo simulations. Improved means that the amplitudes of leading corrections to scaling such as  $b_{\pm}$  in Eq. (1) vanish. The authors of Ref. 18 have studied the high-

TABLE I. Numerical results for the critical exponents  $\nu$ ,  $\gamma$ ,  $\eta$ , and  $\omega$  obtained by using field theoretic methods. The list is by far not exhaustive. We try to give extreme examples; both concerning the values found as well as the quoted error bar. In the case of the  $\epsilon$  expansion we have taken the results that fulfil the boundary condition that for  $\epsilon=2$  the correct two-dimensional Ising results are obtained.

Ref.	Year	Method	$\nu$	$\gamma$	$\eta$	$\omega$
12	1998	$\epsilon$ exp	0.6305(25)	1.2380(50)	0.0365(50)	0.814(18)
13	1991	3D exp	0.630	1.238	0.0355	0.845
11	1991	3D exp	0.6301(5)	1.2378(6)	0.0355(9)	
12	1998	3D exp	0.6304(13)	1.2396(13)	0.0335(25)	0.799(11)
14	1999	3D exp	0.6305	1.241	0.0347(1)	0.805
15	2001	3D exp	0.6303(8)	1.2403(8)	0.0335(6)	0.792(3)
16	2008	3D exp	0.6306(5)	1.2411(6)	0.0318(3)	0.782(5)

temperature series expansion of spin- $S$  Ising models on the simple cubic and the body-centered-cubic lattice up to  $O(\beta^{25})$ . Note that in the spin- $S$  Ising model the spin-variable might assume the values  $-S, -S+1, \dots, S-1, S$ . In Ref. 19 the same authors have studied the  $\phi^4$  model on the simple cubic and the body-centered-cubic lattice also up to  $O(\beta^{25})$ . These results from high-temperature series expansions are all compatible among each other. Note that these expansions were performed for lattice models with quite different Hamiltonians. Furthermore, there are results for both simple cubic and body-centered-cubic lattices. It is highly plausible that corrections to scaling have different amplitudes in these different models. Therefore the agreement of the results gives us confidence that there are no undetected systematic errors due to leading, or in the case of improved models, subleading corrections to scaling. The results for the exponents  $\nu$ ,  $\gamma$ , and  $\eta$  obtained from the high-temperature series expansion are clearly more precise than those obtained by using field-theoretic methods. The results obtained for  $\nu$  using field-theoretic methods and high-temperature series expansions of lattice models are consistent. In the case of  $\gamma$  and  $\eta$  some of the results obtained by resumming the perturbative expansion in three dimensions can be clearly ruled out

by the high-temperature series expansion. Unfortunately, the analysis of the high-temperature series expansions does not provide an accurate estimate for the correction exponent  $\omega$ .

Lattice models can also be studied by using Monte Carlo simulations. The finite size scaling (FSS) approach<sup>25-27</sup> is well suited to locate the critical temperature and to compute critical exponents. Typically one simulates the model directly at the critical point. The critical exponents are then extracted from the scaling of the observables with the lattice size. For example, at the critical temperature the magnetic susceptibility behaves as

$$\chi = aL^{2-\eta} \times (1 + bL^{-\omega} + cL^{-\omega'} + dL^{-2\omega} + \dots) + B, \quad (2)$$

where  $B$  is an analytic background and  $L$  the linear size of a cubic lattice with periodic boundary conditions. An exhaustive summary of previous works is given in Table V of Ref. 4. In Table II we only quote recent works. In 1999 four finite size scaling studies of lattices models in the Ising universality class had been published. The results of these works are consistent among each other and the accuracy that had been achieved is similar to that of the field-theoretic calculations. I like to mention that in Ref. 23 a special purpose computer

TABLE II. Numerical results for the critical exponents  $\nu$ ,  $\gamma$ ,  $\eta$ , and  $\omega$  obtained by analyzing high-temperature (HT) series and Monte Carlo (MC) simulations of lattice models in the Ising universality class. In the case of the MC simulations, some of the authors have quoted the statistical and the systematical errors of  $\nu$  and  $\eta$  separately. The numbers marked by \* are not directly given by the authors but are computed by using the scaling relation  $\gamma = \nu(2 - \eta)$ . Note that the error of  $\gamma$  is computed naively, assuming that the errors of  $\nu$  and  $\eta$  are purely statistical and that the estimates of  $\nu$  and  $\eta$  are uncorrelated. For an exhaustive summary of previous work see Ref. 4.

Ref.	Year	Method	$\nu$	$\gamma$	$\eta$	$\omega$
17	2002	HT	0.63012(16)	1.2373(2)	0.03639(15)	0.825(50)
18	2002	HT	0.6299(2)	1.2371(1)	0.0360(8)*	
19	2005	HT	0.6301(2)	1.2373(2)	0.0363(9)*	
20	1999	MC	0.6294(5) (Ref. 5)	1.2353(21)*	0.0374(6) (Ref. 6)	0.87(9)
21	1999	MC	0.6298(2) (Ref. 3)	1.2365(11)*	0.0366(6) (Ref. 2)	
22	1999	MC	0.6296(3) (Ref. 4)	1.2367(15)*	0.0358(4) (Ref. 5)	0.845(10)
23	1999	MC	0.63032(56)	1.2372(13)*	0.0372(10)	0.82(3)
24	2003	MC	0.63020(12)	1.2372(4)*	0.0368(2)	0.821(5)

for the cluster simulation of the Ising model had been used. In the most recent work,<sup>24</sup> which provides the most accurate estimates so far, 11 different models were studied on lattices up to a linear site of  $L=128$ . The results obtained for  $\nu$ ,  $\gamma$ , and  $\eta$  are essentially consistent with those obtained from the high-temperature series expansions. The estimate obtained for  $\omega$  is more accurate than that of the high-temperature series expansion and it is clearly larger than most of the estimates obtained from the perturbative expansion in three dimensions.

The purpose of the present work is to corroborate the lattice results discussed above. To this end we shall simulate lattices that are considerably larger than those of Ref. 24. Furthermore we shall use improved observables that have been applied in Ref. 28 to study Ising models with quenched dilution. Here, improved means that the amplitude of the leading correction vanishes for any model. Since these observables are constructed numerically, in practice some residual amplitude remains. Using these improved observables in the study of improved models, leading corrections are highly suppressed, allowing us to ignore them in the finite size scaling analysis.

Accurate numerical estimates of critical exponents might serve as benchmark for future experiments, see, e.g., Ref. 6, the analysis of the perturbative expansion in three dimensions, as discussed above, or new theoretical approaches such as new ideas in the so called exact renormalization group<sup>29</sup> or the Kallen-Lehmann approach.<sup>30</sup>

The outline of the paper is the following. First we define the model and the observables that are studied. Then we discuss the Monte Carlo algorithm that has been used. We give the details of our numerical study. We estimate the fixed point values of the phenomenological couplings and the inverse transition temperatures. We give a numerical estimate of the correction exponent  $\omega$  and obtain a new estimate of  $D^*$ , the value of the parameter where leading corrections to scaling vanish. Next we construct various improved observables. Based on this we compute estimates for the critical exponents  $\nu$  and  $\eta$ .

## II. MODEL

The spin-1/2 Ising model is characterized by the reduced Hamiltonian

$$H = -\beta \sum_{\langle xy \rangle} s_x s_y - h \sum_x s_x, \quad (3)$$

where the spin might assume the values  $s_x \in \{-1, 1\}$ .  $x = (x_0, x_1, x_2)$  denotes a site of the simple cubic lattice, where  $x_i \in \{0, 1, 2, \dots, L_i - 1\}$ .  $\langle xy \rangle$  denotes a pair of nearest neighbors on the lattice. We employ periodic boundary conditions in all directions of the lattice. Throughout we shall consider  $L_0 = L_1 = L_2 = L$  and a vanishing external field  $h=0$ . The partition function is given by

$$Z = \sum_{\{s_x\}} \exp(-H), \quad (4)$$

where  $\sum_{\{s_x\}}$  denotes the sum over all configurations.

The Blume-Capel model is characterized by the reduced Hamiltonian

$$H = -\beta \sum_{\langle xy \rangle} s_x s_y + D \sum_x s_x^2 - h \sum_x s_x, \quad (5)$$

where now the spin might assume the values  $s_x \in \{-1, 0, 1\}$ . In the limit  $D \rightarrow -\infty$  the “state”  $s=0$  is completely suppressed, compared with  $s = \pm 1$ , and therefore the spin-1/2 Ising model is recovered. In  $d \geq 2$  dimensions the model undergoes a continuous phase transition for  $-\infty \leq D < D_{tri}$  at a  $\beta_c$  that depends on  $D$ . For  $D > D_{tri}$  the model undergoes a first-order phase transition. References 31–33 give for the three-dimensional simple cubic lattice  $D_{tri} \approx 2.006$ ,  $D_{tri} \approx 2.05$ , and  $D_{tri} = 2.0313(4)$ , respectively.

Numerically it has been shown that on the line of second-order phase transitions there is a point, where leading corrections to scaling vanish. In the following we shall call the model at this point “improved model.” In Ref. 34 we find  $D^* = 0.641(8)$ . One should note that no effort was made to estimate the systematical error due to subleading corrections to scaling. The authors of Refs. 24 and 35 have simulated the model at  $D = \ln 2 = 0.693147\dots$ . At this value of  $D$  corrections to scaling are still small compared with the spin-1/2 Ising model. At  $D = \ln 2$  the Blume-Capel model can be mapped into a spin-1/2 Ising model with twice the number of sites. This model can be simulated with a cluster algorithm without additional local updates as it is the case for general values of  $D$ .

## III. OBSERVABLES

The energy is defined as minus the derivative of the reduced free energy with respect to  $\beta$

$$E = \frac{\partial}{\partial \beta} \ln Z = \sum_{\langle xy \rangle} s_x s_y. \quad (6)$$

This definition is convenient for our purpose. One should note however that it deviates from the standard textbook definition. The magnetic susceptibility  $\chi$  and the second moment correlation length  $\xi_{2nd}$  are defined as

$$\chi \equiv \frac{1}{V} \left\langle \left( \sum_x s_x \right)^2 \right\rangle, \quad (7)$$

where  $V = L^3$  and

$$\xi_{2nd} \equiv \sqrt{\frac{\chi/F - 1}{4 \sin^2 \pi/L}}, \quad (8)$$

where

$$F \equiv \frac{1}{V} \left\langle \left| \sum_x \exp\left(i \frac{2\pi x_k}{L}\right) s_x \right|^2 \right\rangle \quad (9)$$

is the Fourier transform of the correlation function at the lowest nonzero momentum. In our simulations, we have measured  $F$  for the three directions  $k=0, 1, 2$  and have averaged these three results.

In addition to elementary quantities such as the energy, the magnetization, the specific heat, or the magnetic suscep-

tibility, we compute a number of so-called phenomenological couplings, that means quantities that, in the critical limit, are invariant under RG transformations. We consider the Binder parameter  $U_4$  and its sixth-order generalization  $U_6$ , defined as

$$U_{2j} \equiv \frac{\langle m^{2j} \rangle}{\langle m^2 \rangle^j}, \quad (10)$$

where  $m = \frac{1}{V} \sum_x s_x$  is the magnetization of the system. We also consider the ratio  $R_Z \equiv Z_a/Z_p$  of the partition function  $Z_a$  of a system with antiperiodic boundary conditions in one of the three directions and the partition function  $Z_p$  of a system with periodic boundary conditions in all directions. Antiperiodic boundary conditions in the zero direction are obtained by replacing  $s_x s_y$  by  $-s_x s_y$  in the Hamiltonian for links  $\langle xy \rangle$  that connect the boundaries, i.e., for  $x = (L-1, x_1, x_2)$  and  $y = (0, x_1, x_2)$ . The ratio  $Z_a/Z_p$  can be efficiently evaluated using the boundary flip algorithm.<sup>36</sup> Here we use a modified version of the boundary flip algorithm as discussed in Appendix A2 of Ref. 37. In the following we shall refer to the RG-invariant quantities  $U_{2j}$ ,  $R_Z \equiv Z_a/Z_p$  and  $R_\xi \equiv \xi_{2nd}/L$  using the symbol  $R$ .

In our analysis we need the observables as a function of  $\beta$  in some neighborhood of the simulation point. To this end we have computed the coefficients of the Taylor expansion of the observables up to the third order. For example, the first derivative of the expectation value  $\langle A \rangle$  of an observable  $A$  is given by

$$\frac{\partial \langle A \rangle}{\partial \beta} = \langle AE \rangle - \langle A \rangle \langle E \rangle. \quad (11)$$

#### IV. SIMULATION ALGORITHM

Analogous to Ref. 38, we have simulated the Blume-Capel model using a hybrid of local updates and cluster updates. The cluster algorithm only changes the sign of spins. Therefore, in order to get an ergodic algorithm for the Blume-Capel model with finite  $D$ , local Metropolis updates are used that also can change the modulus  $|s_x|$  of the spins. Following Ref. 39 even in the case of the spin-1/2 Ising model such a hybrid of local and cluster updates is superior to the cluster algorithm alone. The authors of Ref. 39 also found that such a hybrid algorithm is much less susceptible to systematic errors caused by the imperfection of pseudorandom numbers than a pure cluster algorithm. Here we have used a hybrid of local Metropolis updates that are implemented by using the multispin coding technique,<sup>40</sup> single cluster updates,<sup>41</sup> and wall cluster updates.<sup>21</sup> In the single cluster update, the cluster that includes a randomly chosen site is flipped. In contrast, in the wall cluster update all clusters that include sites that are part of a given plane (the ‘‘wall’’) of the lattice are flipped.

Motivated by the multispin coding implementation of the local update we have simulated  $N_{bit}=64$  copies of the system in parallel. In the first stage of our study, we have used a single random number sequence for the local Metropolis updates of these  $N_{bit}$  systems. This leads to some degradation of

the performance. To diminish this problem, we have used a modified sequence of the pseudorandom numbers in the second stage of our study. Details are given below. In the case of the cluster updates we could not make use of the multispin coding technique. Therefore we have updated the systems one by one, using different random number sequences for each of the systems.

Let us discuss the implementation of the local Metropolis algorithm in more detail. We have implemented the spin  $s_x \in \{-1, 0, 1\}$  using two bits. To this end we write  $s_x = \sigma_x \tau_x$ , where  $\sigma_x \in \{-1, 1\}$  and  $\tau_x \in \{0, 1\}$ . In terms of these new variables the partition function becomes

$$Z = C \sum_{\{\sigma_x\}} \sum_{\{\tau_x\}} \exp\left(\beta \sum_{\langle xy \rangle} \sigma_x \sigma_y \tau_x \tau_y - \tilde{D} \sum_x \tau_x\right), \quad (12)$$

where  $\tilde{D} = D - \ln 2$ . Note that subtracting  $\ln 2$  corrects for the double counting of the  $s_x = 0$  state.

In our local updating scheme we performed consecutive updates of  $\sigma_x$  and  $\tau_x$ . In the first step, the proposal is given by  $\sigma'_x = -\sigma_x$ . It is accepted with the standard Metropolis acceptance probability

$$P_{acc} = \min\left[1, \exp\left(-2\beta \sigma_x \tau_x \sum_{y.nn.x} \sigma_y \tau_y\right)\right], \quad (13)$$

where  $y.nn.x$  means that  $y$  is a nearest neighbor of  $x$ . In the second step, the proposal is given by  $\tau'_x = 1 - \tau_x$ . A natural choice for the acceptance is

$$P_{acc} = \min\left[1, \exp\left((2\tau_x - 1) \left[-\beta \sigma_x \sum_{y.nn.x} \sigma_y \tau_y + \tilde{D}\right]\right)\right]. \quad (14)$$

Instead, for technical reasons we have implemented a two stage acceptance step. For  $D=0.641$  and  $D=0.655$ , where  $|\tilde{D}|$  is small, we have chosen

$$P_{acc,1} = \min\left[1, \exp\left(\beta(1 - 2\tau_x) \sigma_x \sum_{y.nn.x} \sigma_y \tau_y\right)\right] \quad (15)$$

and

$$P_{acc,2} = \min[1, \exp([2\tau_x - 1]\tilde{D})]. \quad (16)$$

Detailed balance can be easily proven by going through the four cases which are given by positive or negative arguments of the exponential function in Eqs. (15) and (16). We take two uncorrelated random numbers  $r_1$  and  $r_2$  from a uniform distribution in  $[0,1]$ . If both  $P_{acc,1} \geq r_1$  and  $P_{acc,2} \geq r_2$  the proposal is accepted.

In the first stage of our study, we have used the same random number sequence for all  $N_{bit}=64$  systems that we have simulated in parallel. In the second stage of the study, we have used a modified sequence of the random numbers for the acceptance step (13). We have used a 64-bit integer random number in addition to the random number  $r$  that is uniformly distributed in  $[0,1]$ . If the  $i$ th bit of this integer random number is 1 we take  $r$  itself for the acceptance step of the  $i$ th system. Otherwise, if the bit is 0, we take  $1-r$

instead. This modification considerably reduces the correlation among the  $N_{bit}=64$  systems that are simulated in parallel.

We have compared the performance of this local update with that of a local heat bath using a standard implementation. To this end, we have simulated a  $16^3$  lattice at  $\beta=0.3877218$ , which is close to  $\beta_c$  as we shall see below. The integrated autocorrelation times in units of sweeps of the energy density and the magnetic susceptibility are by a factor of about 1.3 larger for the Metropolis update discussed here than for the heat bath update. One sweep over  $N_{bit}=64$  systems in parallel using the multispin coding technique takes about four times as much CPU time as one sweep over a single system using the standard implementation of the heat-bath update. In order to compare the efficiency of the two local updates, we have computed the statistical error of the energy and the magnetic susceptibility, taking into account the possible correlation among the  $N_{bit}=64$  systems in the case of the multispin coding implementation. To this end we have performed a Jackknife analysis, where we have first averaged the measurements of the  $N_{bit}=64$  systems at a given iteration of the Monte Carlo simulation. Taking one over the statistical error squared times the CPU time needed as measure of the efficiency, we find a performance gain of a factor of about 10 of the multispin coding implementation of the local Metropolis update compared with the standard implementation of the heat-bath update.

During the simulation, local Metropolis sweeps, single cluster and wall cluster updates are performed in a certain sequence. In the following we denote an elementary building block of the sequence by cycle. In the case of our most recent simulations ( $D=0.655$ ) such a cycle is composed of (a)  $4\times$  (two Metropolis sweeps followed by  $L/16$  single cluster updates), (b) three Metropolis sweeps, and (c) one wall-cluster update.

In the case of the wall-cluster update we chose the wall to be perpendicular to the 0-, 1-, and 2-axis in three subsequent cycles. The position of the wall along the axis is chosen randomly each time. The parameters of the cycle are chosen such that roughly the same amount of CPU time is spent in each of its three components.

In order to study the performance of the algorithm, we have performed preliminary simulations for  $D=0.655$ , where we have determined the autocorrelation function  $\rho(t)$  of the magnetic susceptibility and the energy density. The statistics of these runs is 300 000 update cycles for the lattice sizes  $L=16, 32, 64$ , and 128 and 82 000 update cycles for  $L=256$  at  $\beta=0.3877218$ , which is close to our final estimate of  $\beta_c$ . The integrated autocorrelation time is given by

$$\tau = \frac{1}{2} + \sum_{t=1}^{t_{max}} \rho(t), \quad (17)$$

where we have chosen  $t_{max}=6\tau$ , self-consistently. Fitting our results for integrated autocorrelation times in units of update cycles we get

$$\tau_\chi = 0.70(4)L^{0.34(1)} \quad (18)$$

for the magnetic susceptibility and

$$\tau_E = 0.47(2)L^{0.42(1)} \quad (19)$$

for the energy density. This means that the autocorrelation times are only a few cycles, even for our largest lattices.

We have estimated the statistical errors of the observables using the Jackknife method. As input of this analysis we have taken data that are already averaged over the  $N_{bit}=64$  systems that are simulated in parallel and might be correlated by the use of a common sequence of random numbers during the Metropolis updates. Therefore the possible correlation among these  $N_{bit}=64$  systems does not affect the correctness of the estimate of the statistical errors.

To figure out how much this correlation does affect the efficiency of the algorithm, we have computed the statistical error, taking only one system, and for comparison, averaging over all  $N_{bit}$  systems. If the simulations were independent, the square of the ratio of these errors, denoted by  $R^2$  in the following, would be equal to  $N_{bit}$ . In fact we see some performance loss due to the use of a common random number sequence. For  $L=16$  we get for the energy density  $R^2 \approx 28.6$  and for the magnetic susceptibility  $R^2 \approx 36.2$ . Fortunately these numbers increase with increasing lattice size. For  $L=256$  we get for the energy density  $R^2 \approx 42.2$  and  $R^2 \approx 48.8$  for the magnetic susceptibility.

In order to give an accurate result for the performance gain that is achieved by using our particular multispin coding implementation of the local update, one would have to tune the parameters of the update cycle for both types of the local update. For lack of time this could not be done. Since the local update is only one of the three components of the complete update cycle, likely the gain is moderate, certainly less than a factor of two.

### Simulations: CPU time and statistics

In a first stage of the study we have simulated the spin-1/2 Ising model and the Blume-Capel model at  $D=0.641, \ln 2, 1.15$ , and 1.5. Note that  $D=0.641$  is the estimate of Ref. 34 for  $D^*$  and  $D=\ln 2$  has been simulated before by the authors of Refs. 24 and 35. At  $D=1.15$  the amplitude of leading corrections to scaling has about the same magnitude as for the spin-1/2 Ising model but opposite sign. A preliminary analysis of these data resulted in  $D^* \approx 0.655$ . Therefore we have simulated at  $D=0.655$  in a second stage of our study.

We have simulated lattices of a linear size  $L$  up to  $L_{max}=96, 200, 360, 300, 64$ , and 48 for the spin-1/2 Ising model and the Blume-Capel model at  $D=0.641, 0.655, \ln 2, 1.15$ , and 1.5, respectively. In Table III we have summarized in detail the lattice sizes that we have simulated and the statistics of these simulations.

In total we have spent the equivalent of 3.5, 9, 16, 3, 3, and 0.1 CPU years on a single core of a Quad-Core AMD Opteron(tm) Processor 2378 running at 2.4 GHz for the spin-1/2 Ising model and the Blume-Capel model at  $D=0.641, 0.655, \ln 2, 1.15$ , and 1.5, respectively.

As random number generator we have used the SIMD-oriented (single instruction multiple data) fast Mersenne Twister algorithm.<sup>42</sup> As a check we have repeated our simulations at  $D=0.655$  using the WELL random number generator<sup>43</sup> with about one third of the statistics reported in

TABLE III. We give the number of update-cycles divided by  $64 \times 15\,000$  as a function of the lattice size and the value of the parameter  $D$ . For a discussion see the text.

$L$	Ising	0.641	0.655	ln 2	1.15	1.5
10	10000	10000	4005		10000	
11			4005			
12	9593	20000	4000	4083	10000	1000
13			4005			
14	11747	10000	4005	3003	10000	
15			3994			
16	9740	20200	3999	2371	9917	1000
17			4000			
18	11524	10000	3993	1807	11102	
20	6959	12000	3995	1828	7208	
22	11320		4003	1813	12328	
24	12000	10971	4000	2471	13239	1000
28	4374	7024	3999	2920	5420	
32	5091	2291	3011	2533	4582	692
36	3951	3362			3444	
40	1658	2349	1657	1466	1474	
48	1890	2202			1502	206
50			968	624		
56	629	824			688	
64	719	697	286		485	
70			894			
72		848				
80		1053				
96	273					
100		753	435			
128			136			
150		319	179			
200		149	106			
250			118	58		
300			62	14		
360			11			

Table III. In particular, we have used the program WELL44497A.C provided by the authors. We found that the estimates of individual observables are consistent. We have also repeated part of the finite size scaling analysis using these data. For given ansätze we found consistent, even though less precise results for the critical exponents. One should note that the statistical error of the fit parameters is often much smaller than the final error that also includes systematical errors due to subleading corrections. The following analysis is only based on the simulations using the Mersenne Twister algorithm.<sup>42</sup>

### V. $\beta_c$ AND THE FIXED POINT VALUES OF PHENOMENOLOGICAL COUPLINGS

In a first step of the analysis we have studied the finite size scaling behavior of the phenomenological couplings at  $D=0.655$  since here we have accumulated the best statistics

and second, as we shall see below, this value of  $D$  is closest to  $D^*$  among the values that we have simulated.

At the critical point a phenomenological coupling behaves as

$$R(L, \beta_c) = R^* + aL^{-\omega} + bL^{-\omega'} + cL^{-2\omega} + \dots, \quad (20)$$

where  $\omega \approx 0.8$  as discussed in Sec. I. Below we shall find  $\omega=0.832(6)$ . The subleading corrections exponent is  $\omega' = 1.67(11)$ .<sup>44</sup> Furthermore, there should be corrections with  $\omega' \approx 2$  due to the breaking of the rotational symmetry by the lattice<sup>45</sup> or due to the analytic background of the magnetic susceptibility. Motivated by Eq. (20), we have fitted our data with three different ansätze

$$R(L, \beta_c) = R^*, \quad (21)$$

$$R(L, \beta_c) = R^* + aL^{-\epsilon_1}, \quad (22)$$

TABLE IV. Fitting the data for  $Z_a/Z_p$  obtained at  $D=0.655$  with the ansätze (21)–(23).  $L_{\min}$  is the minimal lattice size that is included into the fit. For a discussion see the text.

Ansatz	$\epsilon_1$	$\epsilon_2$	$L_{\min}$	$\beta_c$	$(Z_a/Z_p)^*$	$\chi^2/\text{d.o.f.}$
(21)			32	0.387721745(10)	0.542489(14)	9.5/10
(22)	0.83		18	0.387721730(12)	0.542589(33)	12.4/14
(22)	1.6		12	0.387721729(10)	0.542558(12)	24.0/20
(22)	2		10	0.387721734(10)	0.542532(8)	27.4/22
(23)	0.83	1.6	10	0.387721746(12)	0.542448(46)	27.6/21
(23)	0.83	2	10	0.387721740(12)	0.542502(38)	26.8/21

$$R(L, \beta_c) = R^* + aL^{-\epsilon_1} + bL^{-\epsilon_2}, \quad (23)$$

where we have used in Eq. (22) the choices  $\epsilon_1=0.83$ ,  $\epsilon_1=1.6$ , or  $\epsilon_1=2$  and in Eq. (23)  $\epsilon_1=0.83$  and  $\epsilon_2=1.6$  or  $\epsilon_2=2$ . Here and in the following ansätze, we denote a correction exponent with a fixed value by  $\epsilon$ . Instead, if it is a free parameter we shall denote it, as usual, by  $\omega$ . Here we need the phenomenological couplings  $R$  as a function of the inverse temperature. To this end we have used the Taylor expansion around the value  $\beta_s$  of the inverse temperature that we have used in the simulation. We have checked that the result for  $\beta_c$  and  $\beta_s$  are sufficiently close to avoid significant truncation effects. This way, for example Eq. (21) becomes

$$R(L, \beta_s) = R^* - c_1(L, \beta_s)(\beta_c - \beta_s) - \frac{c_2(L, \beta_s)}{2!}(\beta_c - \beta_s)^2 - \frac{c_3(L, \beta_s)}{3!}(\beta_c - \beta_s)^3, \quad (24)$$

where  $R^*$  and  $\beta_c$  are the two parameters of the fit. Since we have chosen  $\beta_s$  as a good approximation of  $\beta_c$ , we could ignore the relatively small statistical error of the Taylor coefficients  $c_1$ ,  $c_2$ , and  $c_3$ , which simplifies the fit.

As an example let us discuss the results obtained for  $Z_a/Z_p$  in more detail. A selection of our results is given in Table IV. We have fitted the data for all linear lattice sizes  $L$  that are larger than or equal to a certain  $L_{\min}$ . Starting from the  $L_{\min}$  given in column 5 of Table IV the  $\chi^2/\text{d.o.f.}$  is close to one.

Taking into account the variation in the results over the different ansätze we arrive at our final estimate  $\beta_c = 0.38772174(2)$  and  $(Z_a/Z_p)^* = 0.5425(1)$ . We performed a similar analysis for  $\xi_{2nd}/L$ ,  $U_4$ , and  $U_6$ . Our final results are summarized in Table V. We find that the estimates of  $\beta_c$

TABLE V. Results for the inverse critical temperature  $\beta_c$  at  $D=0.655$  obtained from the FSS study of various phenomenological couplings. In addition we give the fixed point values  $R^*$  of these quantities. For a discussion see the text.

	$Z_a/Z_p$	$\xi_{2nd}/L$	$U_4$	$U_6$
$\beta_c$	0.38772174(2)	0.38772174(2)	0.38772173(2)	0.38772173(2)
$R^*$	0.5425(1)	0.6431(1)	1.6036(1)	3.1053(5)

obtained from different phenomenological couplings are consistent within error bars. We take the average

$$\beta_c = 0.387721735(25) \quad (25)$$

as our final estimate of the inverse critical temperature. The error bar is chosen such that it covers all results given in Table V, including their error bars.

Our result for  $U_4^*$  is about three times the combined error smaller than  $U_4^* = 1/0.62341(4) = 1.60408(10)$  given in Ref. 24. We regard our result as more reliable since we have simulated larger lattices and have carefully estimated systematic errors due to subleading corrections that are not included into the fit.

In the case of the other models we also determined  $\beta_c$  by fitting with the ansätze [Eqs. (21)–(23)]. Here however we have used the results for  $(Z_a/Z_p)^*$ ,  $(\xi_{2nd}/L)^*$ ,  $U_4^*$  and  $U_6^*$  given in Table V as input. The final results obtained this way are summarized in Table VI. For completeness we have included the results for  $D=0.655$  given in Eq. (25). Our result for  $\beta_c$  of the spin-1/2 Ising model is fully consistent with  $\beta_c = 0.22165455(3)$  given in Ref. 24. For a summary of previous results for  $\beta_c$  of the spin-1/2 Ising model we refer the reader to Table I of Ref. 34. Our result for  $\beta_c$  at  $D=\ln 2$  is by 1.5 times the combined error larger than  $\beta_c = 0.39342225(5)$  given in Ref. 24.

## VI. THE CORRECTION EXPONENT $\omega$ AND THE IMPROVED MODEL

In this section we study the cumulants  $U_4$  and  $U_6$  at a fixed value of  $Z_a/Z_p$  or  $\xi_{2nd}/L$ . To this end one determines the inverse temperature  $\beta_f(L)$  defined by

TABLE VI. Estimates of the inverse critical temperature  $\beta_c$  of the spin-1/2 Ising model and the Blume-Capel model at various values of  $D$ . For a discussion see the text.

$D$	$\beta_c$
Ising	0.22165463(8)
0.641	0.38567122(5)
0.655	0.387721735(25)
$\ln 2 = 0.69314718\dots$	0.39342239(8)
1.15	0.4756110(2)
1.5	0.5575303(10)

$$R_1(L, \beta_f(L)) = R_{1,f}, \quad (26)$$

where  $R_1$  is either  $Z_a/Z_p$  or  $\xi_{2nd}/L$  and  $R_{f,1}$  the required value. As  $R_{f,1}$  we take the fixed point values of  $Z_a/Z_p$  and  $\xi_{2nd}/L$  obtained above. We define

$$\bar{R}_2(L) \equiv R_2(L, \beta_f(L)), \quad (27)$$

where  $R_2$  is, in our case, either  $U_4$  or  $U_6$ . In the following we shall denote  $\bar{R}_2$  by  $R_2$  at  $R_1=R_{1,f}$ . In practice we have done these calculations using the Taylor expansion of  $R_1$  and  $R_2$  around the value  $\beta_s$  that we have used in the simulation up to third order. We have checked carefully that  $\beta_s$  and  $\beta_f$  are sufficiently close to avoid significant truncation errors.

One finds, see, e.g., Sec. III of Ref. 37

$$\begin{aligned} \bar{R}(D, L) = & \bar{R}^* + a(D)L^{-\omega} + b(D)L^{-\omega'} + \dots + ca^2(D)L^{-2\omega} \\ & + \dots, \end{aligned} \quad (28)$$

where we should note that the correction amplitudes depend on the parameter  $D$  of our model. The improved model is characterized by a vanishing amplitude of leading corrections to scaling. Hence  $D^*$  is given by the zero of  $a(D)$ . We have analyzed the data of five different models in combined fits: The Ising model and the Blume-Capel model at  $D=0.641$ ,  $D=0.655$ ,  $D=\ln 2$ , and  $D=1.15$ . To this end we have employed various ansätze that are derived from Eq. (28),

$$\bar{R}(D, L) = \bar{R}^* + a(D)L^{-\omega}, \quad (29)$$

$$\bar{R}(D, L) = \bar{R}^* + a(D)L^{-\omega} + ca^2(D)L^{-2\omega}, \quad (30)$$

$$\bar{R}(D, L) = \bar{R}^* + a(D)L^{-\omega} + ca^2(D)L^{-2\omega} + bL^{-\epsilon}, \quad (31)$$

$$\bar{R}(D, L) = \bar{R}^* + a(D)L^{-\omega} + ca^2(D)L^{-2\omega} + da^3(D)L^{-3\omega}, \quad (32)$$

$$\bar{R}(D, L) = \bar{R}^* + a(D)L^{-\omega} + ca^2(D)L^{-2\omega} + da^3(D)L^{-3\omega} + bL^{-\epsilon}. \quad (33)$$

In the ansatz (29) the free parameters of the fit are  $\bar{R}^*$ ,  $a$ (Ising),  $a$ (0.641),  $a$ (0.655),  $a$ ( $\ln 2$ ),  $a$ (1.15) and the correction exponent  $\omega$ . In the ansatz (30) we have in addition the parameter  $c$ . In the ansatz (31) we have added the term  $bL^{-\epsilon}$  to take subleading corrections into account. Here we make the approximation that the parameter  $b$  is model independent. We fix the subleading correction exponent  $\epsilon=1.6$  or  $\epsilon=2$ . In the ansatz (32) we take into account corrections  $\propto L^{-3\omega}$ . Finally in the ansatz (33) we add, similar to Eq. (31) a term  $bL^{-\epsilon}$ .

In the case of the ansatz (29) fits with  $\chi^2/\text{d.o.f.} < 2$  are only obtained for  $L_{\min} \geq 36$ . Instead, fitting with ansatz (30) we get for  $U_4$  at  $Z_a/Z_p=0.5425$   $\chi^2/\text{d.o.f.}=62.4/62$  already for  $L_{\min}=16$ . The results for the parameters of this fit are  $\omega=0.832(1)$ ,  $\bar{U}_4^*=1.60357(1)$ ,  $a$ (Ising)=-0.2983(6),  $a$ (0.641)=-0.0067(2),  $a$ (0.655)=-0.0006(2),  $a$ ( $\ln 2$ )=0.0167(2),  $a$ (1.15)=0.380(1), and  $c=2.08(3)$ . Note that here and in the

following the errors quoted for results of individual fits are purely statistical. Extrapolating  $a$ (0.641) and  $a$ (0.655) we get  $D^*=0.6564(5)$ .

We estimated the systematic error due to corrections that are not taken into account in the ansatz (30) from the variation of the results obtained with the ansätze (31)–(33) and by using  $U_6$  instead of  $U_4$ . Furthermore we have redone the analysis for  $U_4$  and  $U_6$  at  $\xi_{2nd}/L=0.6431$ . We arrive at the final estimates

$$\omega = 0.832(6), \quad (34)$$

$$D^* = 0.656(20). \quad (35)$$

It also follows from the fits that the amplitude of corrections to scaling at  $D=0.655$  is at least by a factor of 30 smaller than that of the spin-1/2 Ising model.

## VII. IMPROVED OBSERVABLES

The exponent  $\nu$  can be obtained from the behavior of the slope of a phenomenological coupling at the critical point

$$\left. \frac{\partial R}{\partial \beta} \right|_{\beta=\beta_c} = aL^{1/\nu}(1 + bL^{-\omega} + \dots). \quad (36)$$

The exponent  $\eta$  can be extracted from the behavior of the magnetic susceptibility at the critical point

$$\chi|_{\beta=\beta_c} = aL^{2-\eta}(1 + bL^{-\omega} + \dots). \quad (37)$$

Note that the coefficients  $a$  and  $b$  of course take different values in Eqs. (36) and (37). Such a procedure requires an estimate of  $\beta_c$ . To avoid this we have studied, following Ref. 22, the slopes and the magnetic susceptibility at  $\beta_f$  as defined in Eq. (26). These quantities behave as

$$\frac{\partial \bar{R}}{\partial \beta} \equiv \left. \frac{\partial R}{\partial \beta} \right|_{\beta=\beta_f} = a(D)L^{1/\nu}(1 + b(D)L^{-\omega} + \dots) \quad (38)$$

and

$$\bar{\chi} \equiv \chi|_{\beta=\beta_f} = a(D)L^{2-\eta}(1 + b(D)L^{-\omega} + \dots). \quad (39)$$

Again we have computed these quantities using their Taylor expansion around  $\beta_s$  up to the third order.

Here, following Ref. 28, we shall study improved versions of the slopes and the magnetic susceptibility. This means in the ideal case that the amplitude of leading corrections vanishes for any model. In practice, as we shall see below, we can construct quantities for that the amplitude of leading corrections is suppressed by more than one order of magnitude. Using such quantities in the case of improved models ensures that leading corrections to scaling are suppressed by two to three orders of magnitude compared with standard observables in the case of, e.g., the spin-1/2 Ising model. This is sufficient to ignore leading corrections to scaling in the analysis of our data.

Let us discuss in detail the construction of the improved observable at the example of the magnetic susceptibility. We consider



$$\bar{\chi}_{imp}(L,D) = \bar{U}_4(L,D)^x \bar{\chi}(L,D), \quad (40)$$

where  $x$  is chosen such that the amplitude of leading corrections vanishes. Note that instead of  $\bar{U}_4$  also  $\bar{U}_6$  could be used. It is important to take a phenomenological coupling, where leading corrections to scaling are clearly visible. Let us recall the finite size scaling behavior of the Binder cumulant

$$\bar{U}_4(L,D) = \bar{U}_4^* + b_U(D)L^{-\omega} + \dots \quad (41)$$

Inserting Eqs. (39) and (41) into Eq. (40) we get

$$\bar{\chi}_{imp}(L,D) = a(D)\bar{U}_4^x L^{2-\eta} \left( 1 + \left[ b(D) + x \frac{b_U(D)}{\bar{U}_4^*} \right] L^{-\omega} + \dots \right). \quad (42)$$

Hence the exponent defining the improved observable is given by

$$x = -b(D) \frac{\bar{U}_4^*}{b_U(D)}. \quad (43)$$

Note that ratios of correction amplitudes are universal. Therefore the exponent  $x$  does not depend on  $D$ . It can be best determined by analyzing data obtained for models with relatively large corrections to scaling. For example, one might consider the spin-1/2 Ising model to this end. We have already determined  $b_U(\text{Ising})$  and  $\bar{U}_4^*$  in the previous section. In order to obtain  $b(D)$  one would fit  $\bar{\chi}(L,D)$  with ansätze motivated by Eq. (39).

However it turns out to be more efficient to study ratios of observables taken from two different models. This way, critical exponents cancel and therefore fits have less parameters and become more reliable. In particular, we shall study the spin-1/2 Ising model and the Blume-Capel at  $D=1.15$ . We define

$$\begin{aligned} R_\chi(L) &= \frac{\bar{\chi}(L, \text{Ising})}{\bar{\chi}(L, D=1.15)} \\ &= \frac{a(\text{Ising})}{a(D=1.15)} (1 + [b(\text{Ising}) - b(1.15)]L^{-\omega} + \dots) \end{aligned} \quad (44)$$

and

$$R_U(L) = \frac{\bar{U}(L, \text{Ising})}{\bar{U}(L, D=1.15)} = 1 + \frac{b_U(\text{Ising}) - b_U(1.15)}{\bar{U}^*} L^{-\omega} + \dots, \quad (45)$$

where now

$$x = -[b(\text{Ising}) - b(1.15)] \frac{\bar{U}^*}{b_U(\text{Ising}) - b_U(1.15)}. \quad (46)$$

The exponent  $x$  can be directly obtained from fits with the ansatz

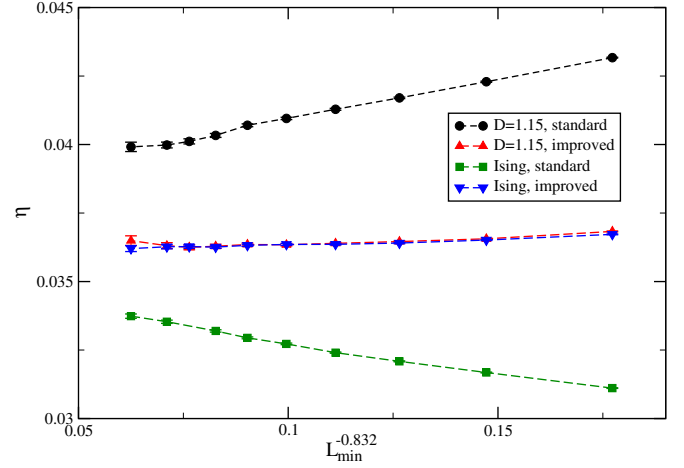


FIG. 1. (Color online) Results for the critical exponent  $\eta$  obtained by fitting the standard and the improved magnetic susceptibility at  $Z_a/Z_p=0.5425$  for the Ising model and the Blume-Capel model at  $D=1.15$  using the ansatz (49).  $L_{min}$  is the minimal lattice size that is taken into account. In the case of the improved magnetic susceptibility, the results obtained from the two different models fall nicely on top of each other. The dashed lines should only guide the eyes.

$$R_U(L)^x R_\chi(L) = C, \quad (47)$$

where  $x$  and  $C$  are the parameters of the fit. To check for the effect of subleading corrections we have also fitted the data with the ansatz

$$R_U(L)^x R_\chi(L) = C + cL^{-\epsilon}, \quad (48)$$

where  $c$  is an additional parameter and we have fixed either  $\epsilon=1.6$  or  $\epsilon=2$ . Fixing  $Z_a/Z_p=0.5425$ , fits with the ansatz (47) have an  $\chi^2/\text{d.o.f.} \approx 1$  starting with  $L_{min}=16$ . Using  $L_{min}=16$  we get  $x=-0.656(1)$ . Instead using the ansatz (48) we get  $\chi^2/\text{d.o.f.} \approx 1$  already for  $L_{min}=10$ . The results for  $L_{min}=10$  are  $x=-0.665(2)$  and  $x=-0.661(2)$  for  $\epsilon=1.6$  and  $\epsilon=2$ , respectively. As our final result we quote  $x=-0.66(1)$ , where the error is chosen such that it covers the three estimates given above. In a similar fashion we arrive at  $x=-0.57(2)$  for fixing  $\xi_{2nd}/L=0.6431$ .

In Fig. 1 we demonstrate the effectiveness of the improvement. We have analyzed our data for  $\chi$  at  $Z_a/Z_p=0.5425$  for the Ising model and the Blume-Capel model at  $D=1.15$ . To this end, we have fitted our data with the ansatz

$$\bar{\chi} = aL^{2-\eta} + B, \quad (49)$$

where  $B$  is an analytic background.

Using the standard magnetic susceptibility, we get  $\chi^2/\text{d.o.f.}=4.6/4$  for  $L_{min}=32$  in the case of the Ising model and  $\chi^2/\text{d.o.f.}=2.6/5$  for  $L_{min}=24$  in the case of the Blume-Capel model at  $D=1.15$ . Nevertheless for, e.g.,  $L_{min}=32$  the results for  $\eta$  obtained from the two different models differ by more than 20 standard deviations. In contrast, for the improved magnetic susceptibility the results obtained for the two models are quite similar. In particular, for  $L_{min}=24$  the

TABLE VII. Exponent  $x$  of improved slopes as defined by Eq. (50). In the first column we give the phenomenological coupling and its value that is used to define  $\beta_f$ . In the first row we give the quantity whose slope is considered. For a discussion see the text.

Fix; slope of	$Z_a/Z_p$	$\xi_{2nd}/L$	$U_4$	$U_6$
$Z_a/Z_p=0.5425$	0.52(2)	0.77(3)	-1.21(5)	-2.73(5)
$\xi_{2nd}/L=0.6431$	0.54(2)	0.81(2)	-1.21(3)	-2.71(4)

estimates for  $\eta$  obtained from the Ising model and the Blume-Capel model at  $D=1.15$  are consistent within the error bars.

We also have constructed improved slopes

$$\bar{S}_{imp}(L,D) = \bar{U}_4(L,D)^x \bar{S}(L,D), \quad (50)$$

where  $x$  is chosen such that leading corrections to scaling vanish. We have determined  $x$  analogous to the case of the magnetic susceptibility discussed above. To this end we have computed the ratios

$$R_S(L) = \frac{\bar{S}(L, \text{Ising})}{\bar{S}(L, D=1.15)}. \quad (51)$$

As discussed above for the case of the magnetic susceptibility, we have fitted

$$R_U(L)^x R_S(L) = C \quad (52)$$

with  $x$  and  $C$  as free parameters and, as check

$$R_U(L)^x R_S(L) = C + cL^{-\epsilon}, \quad (53)$$

where  $c$  is an additional parameter and  $\epsilon$  is fixed to either 1.6 or 2. Our final results for the exponent  $x$  are summarized in Table VII.

Furthermore we have constructed quantities of the type

$$\bar{S}_{ij} = |\bar{S}_i|^x |\bar{S}_j|^{1-x}, \quad (54)$$

where  $x$  is again chosen such that the amplitude of the leading correction vanishes. Here we performed fits with the ansatz

$$R_{S_i}^x R_{S_j}^{1-x} = C, \quad (55)$$

where  $x$  and  $C$  are the parameters of the fit and

TABLE VIII. Exponent  $x$  of improved slopes as defined by Eq. (54). In the first column we give the phenomenological coupling and its value that is used to define  $\beta_f$ . In the first row we give the quantity whose slope is mixed with that of  $\bar{U}_4$ . For a discussion see the text.

Fix; slope of	$Z_a/Z_p$	$\xi_{2nd}/L$
$Z_a/Z_p=0.5425$	0.29(1)	0.39(1)
$\xi_{2nd}/L=0.6431$	0.31(1)	0.41(1)

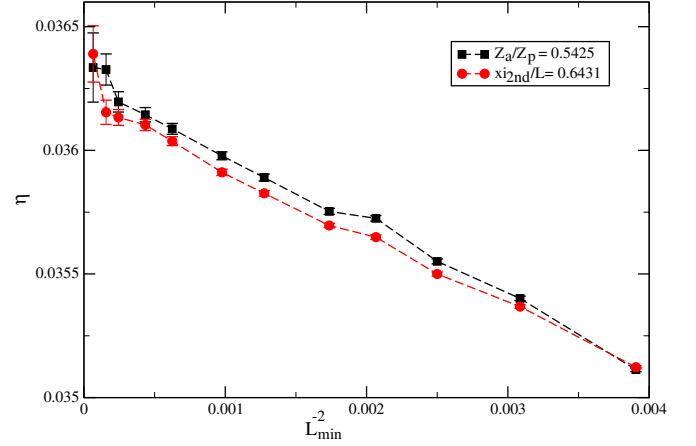


FIG. 2. (Color online) Results for the critical exponent  $\eta$  obtained by fitting the improved magnetic susceptibility at  $Z_a/Z_p=0.5425$  and at  $\xi_{2nd}/L=0.6431$  using the ansatz (57). Data for the Blume-Capel model at  $D=0.641$  and  $D=0.655$  are taken into account.  $L_{min}$  is the minimal lattice size that is taken into account. The dashed lines should only guide the eyes. For a discussion see the text.

$$R_{S_i}^x R_{S_j}^{1-x} = C + cL^{-\epsilon} \quad (56)$$

with the additional parameter  $c$ . Also here we have fixed either  $\epsilon=1.6$  or  $\epsilon=2$ . In practice we have combined the slope of  $U_4$  with the slope of  $Z_a/Z_p$  or  $\xi_{2nd}/L$ . Our results for the exponent  $x$  are summarized in Table VIII. Notice that the results obtained for  $Z_a/Z_p=0.5425$  and  $\xi_{2nd}/L=0.6431$  are similar but not identical.

### VIII. EXPONENT $\eta$

We have fitted our data for the improved magnetic susceptibility at  $Z_a/Z_p=0.5425$  and  $\xi_{2nd}/L=0.6431$  using the ansätze

$$\bar{\chi}_{imp} = a(D)L^{2-\eta}, \quad (57)$$

$$\bar{\chi}_{imp} = a(D)L^{2-\eta} + B(D), \quad (58)$$

$$\bar{\chi}_{imp} = a(D)L^{2-\eta}[1 + d(D)L^{-\epsilon}]. \quad (59)$$

In the ansatz (58) we have taken into account the analytic background  $B$  of the magnetic susceptibility. Since  $\eta$  is small, the parameter  $B$  also takes effectively into account other corrections that have a correction exponent  $\omega'' \approx 2$  like for example the breaking of the rotational symmetry by the lattice. In the ansatz (59) we have set  $\epsilon=1.6$ . Using this ansatz we try to estimate the possible effect of a correction caused by  $\omega'=1.67(11)$  (Ref. 44) on our estimate of  $\eta$ .

We have fitted the data for  $D=0.641$  and  $D=0.655$  in a common fit. The parameters of these fits are  $a(0.641)$ ,  $a(0.655)$ , and  $\eta$  in the case of the ansatz (57) and in addition  $B(0.641)$  and  $B(0.655)$  or  $d(0.641)$  and  $d(0.655)$  in the case of the ansatz (58) and (59), respectively. In Fig. 2 we have plotted estimates of  $\eta$  obtained by fitting with the ansatz (57) as a function of  $L_{min}^{-2}$ . Up to  $L_{min}=48$  the results fall roughly

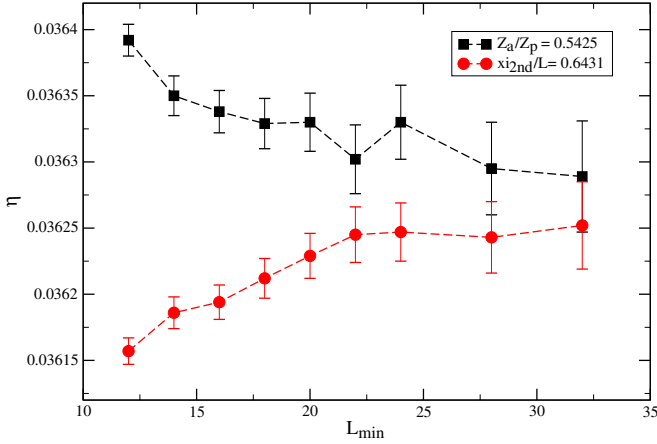


FIG. 3. (Color online) Results for the critical exponent  $\eta$  obtained by fitting the improved magnetic susceptibility at  $Z_a/Z_p = 0.5425$  and at  $\xi_{2nd}/L = 0.6431$  using the ansatz (58). Data for the Blume-Capel model at  $D=0.641$  and  $D=0.655$  are taken into account.  $L_{min}$  is the minimal lattice size that is taken into account. The dashed lines should only guide the eyes. For a discussion see the text.

on a straight line, indicating that corrections with an exponent  $\epsilon \approx 2$  are present. For  $L_{min}=128$  one finds that  $\chi^2/\text{d.o.f.}$  is smaller than one for both taking the improved susceptibility at  $Z_a/Z_p=0.5425$  and  $\xi_{2nd}/L=0.6431$ . The estimate  $\eta = 0.03636(20)$  covers both results obtained at  $L_{min}=128$ , including their error bars.

Next we have fitted our data with the ansatz (58). For both the improved magnetic susceptibility at  $\xi_{2nd}=0.6431$  and at  $Z_a/Z_p=0.5425$  we get  $\chi^2/\text{d.o.f.} < 2$  starting from  $L_{min}=14$ . The results for  $\eta$  are plotted in Fig. 3. In the case of  $\xi_{2nd}=0.6431$  the estimate of  $\eta$  is increasing with increasing  $L_{min}$  while it is decreasing for  $Z_a/Z_p=0.5425$ . For  $L_{min}=32$  the two results are consistent within error bars.

We read off our final estimate

$$\eta = 0.03627(10). \quad (60)$$

The error estimate is chosen such that it also covers results obtained with the ansatz (59) and  $L_{min}=32$ .

### IX. CRITICAL EXPONENT $\nu$

In order to determine the exponent  $\nu$  we performed combined fits of our data for the improved slopes at  $D=0.641$  and  $D=0.655$ . In a first step of the analysis we have fitted the improved slopes with a power law without any correction

$$\bar{s}_{imp} = a(D)L^{1/\nu}, \quad (61)$$

where the amplitudes  $a(0.641)$ ,  $a(0.655)$  and the exponent  $\nu$  are the parameters of the fit. In Fig. 4 we give the results for  $\nu$  as a function of  $L_{min}^{-2}$ , where  $L_{min}$  is the minimal lattice size that is included into the fit. In the figure we give only results for taking the slopes at  $Z_a/Z_p=0.5425$ . Those for the slopes at  $\xi_{2nd}/L=0.6431$  behave in a very similar way.

We find that the result for  $\nu$  obtained from the improved slope of  $Z_a/Z_p$  is increasing with increasing  $L_{min}$  while the

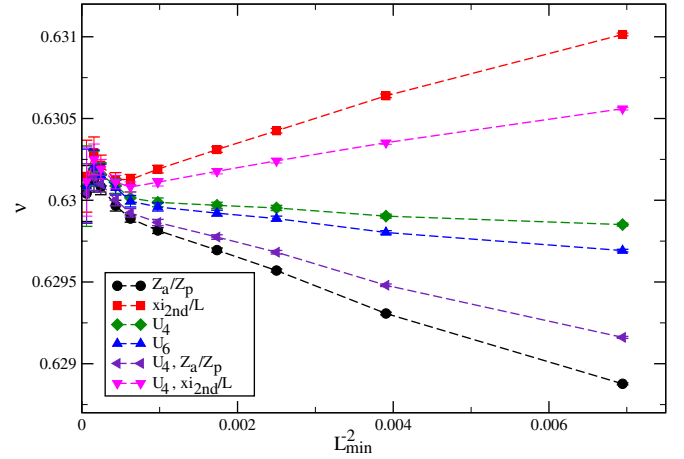


FIG. 4. (Color online) Results for the critical exponent  $\nu$  obtained by fitting improved slopes of various phenomenological couplings at  $Z_a/Z_p=0.5425$  as a function of  $L_{min}^{-2}$ , where  $L_{min}$  is the minimal lattice size that is included into the fit. The dashed lines should only guide the eyes. For a discussion see the text.

one obtained from  $\xi_{2nd}/L$  is decreasing. The results obtained from the improved slope of  $U_4$  and  $U_6$  are quite similar. They only slightly increase with increasing  $L_{min}$ . We have also plotted results obtained from the combined slopes [Eq. (54)]. In the case of combining the slope of  $U_4$  with that of  $\xi_{2nd}/L$  the estimate of  $\nu$  is decreasing with increasing  $L_{min}$  while for combining the slope of  $U_4$  with that of  $Z_a/Z_p$  it is increasing. In all cases a rather large  $L_{min}$  is needed to get acceptable values for  $\chi^2/\text{d.o.f.}$  In the worst case, for the improved slope of  $Z_a/Z_p$  only for  $L_{min} \geq 56$  a  $\chi^2/\text{d.o.f.}$  smaller than two is reached. The behavior of the estimates of  $\nu$  for  $L_{min} < 48$  is consistent with the fact that the dominating corrections have an exponent  $\omega' \approx 2$ . For larger  $L_{min}$ , the variation of our estimates of  $\nu$  with  $L_{min}$  seems to be dominated by statistical fluctuations. For  $L_{min}=128$  we get  $\chi^2/\text{d.o.f.}$  smaller than one for all quantities that we have considered. The estimate  $\nu = 0.6301(3)$  covers the results, including the statistical error, of all our fits for  $L_{min}=128$ . Note that in Ref. 24  $L=128$  is the largest lattice size that is simulated.

Motivated by these observations, we have fitted our data with the ansatz

$$\bar{s}_{imp} = a(D)L^{1/\nu} \times (1 + bL^{-\epsilon}), \quad (62)$$

where we have fixed  $\epsilon$  to either 1.6 or 2. Since already  $a(0.641)$  and  $a(0.655)$  are very similar, we have chosen the parameter  $b$  to be model independent. Let us first discuss the fits with  $\epsilon=2$ . Such fits give  $\chi^2/\text{d.o.f.}$  close to one already for  $L_{min}=10$ . In the lower part of Fig. 5 we have plotted the results obtained from the slopes of different quantities for  $10 \leq L_{min} \leq 24$ . These different estimates of  $\nu$  are consistent among each other. Furthermore there is little variation in the results with  $L_{min}$ .

In the upper part of Fig. 5 we plot the corresponding result for  $\epsilon=1.6$ . Here the  $\chi^2/\text{d.o.f.}$  is somewhat larger than for  $\epsilon=2$ . Also the result for  $\nu$  clearly depends on the quantity that is analyzed. We conclude that the numerically dominant corrections have an exponent  $\epsilon \approx 2$ . Motivated by these fits,

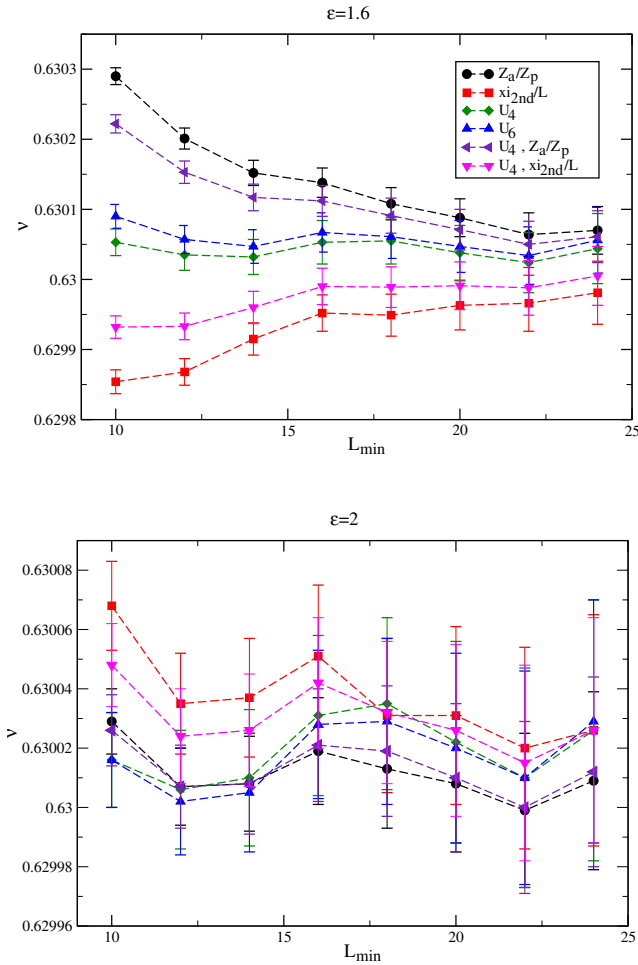


FIG. 5. (Color online) Results for the critical exponent  $\nu$  obtained by fitting improved slopes of various phenomenological couplings at  $Z_a/Z_p=0.5425$  with the ansatz (62) as a function of  $L_{min}$ . In the upper part of the figure the correction exponent is fixed to  $\epsilon=1.6$  and in the lower part it is fixed to  $\epsilon=2$ . The dashed lines should only guide the eyes. For a discussion see the text.

we take  $\nu=0.63002$  as our final result. Since we cannot exclude that there are also corrections with an exponent  $\epsilon \approx 1.6$ , we take these fits into account in our final error of  $\nu$ . For  $L_{min}=22$  and  $L_{min}=24$  all results that we have obtained with the ansatz (62), including their error bar, are contained in the interval  $[0.62992, 0.63012]$ . Therefore we quote as our final result

$$\nu = 0.63002(10). \quad (63)$$

## X. SUMMARY AND CONCLUSIONS

We have simulated the spin-1/2 Ising model and the Blume-Capel model on the simple cubic lattice using linear lattice sizes  $L \leq 360$ . Using finite size scaling methods we have determined critical properties of the models. In particular, we have determined the value  $D^*=0.656(20)$  of the parameter  $D$  of the Blume-Capel model, where leading corrections to scaling vanish. We have accurately determined the inverse of the critical temperature for various values of  $D$ ,

in particular,  $\beta_c(0.641)=0.38567122(5)$  and  $\beta_c(0.655)=0.387721735(25)$ . We have computed the critical exponents  $\nu=0.63002(10)$  and  $\eta=0.03627(10)$  as well as the exponent  $\omega=0.832(6)$  of leading corrections to scaling. The errors quoted for these final results cover statistical as well as systematical errors. Systematical errors are due to the fact that power laws like Eqs. (36) and (37) that govern the finite size scaling behavior of physical quantities at the critical temperature are subject to an infinite series of correction terms. Fitting Monte Carlo data, only few of these correction terms can be taken into account. In the present study, we have effectively eliminated the leading correction  $\propto L^{-\omega}$  by simulating an improved model and analyzing improved observables as discussed in Sec. VII. In our ansätze we take into account a subleading correction with the exponent  $\omega'=1.67(11)$  predicted by Ref. 44 or  $\omega' \approx 2$  due to the breaking of the rotational symmetry by the simple cubic lattice<sup>45</sup> or due to the analytic background of the magnetic susceptibility. We estimate the error caused by correction terms that are not included by comparing the results obtained by using different ansätze and, even more important, by fitting different quantities. One expects that in the generic case the amplitudes of corrections are different for different quantities. In the case of the critical exponent  $\nu$  we have studied the slope of four different phenomenological couplings: The cumulants  $U_4$  and  $U_6$ , the ratio of partition functions  $Z_a/Z_p$ , and the second moment correlation length over the linear lattice size  $\xi_{2nd}/L$ . We regard the estimates of the error obtained this way as quite robust and therefore the results obtained here should serve well as benchmark for experimental studies as well as new or developing theoretical methods.

Our results are fully consistent with those obtained from high-temperature series expansion of lattice models;<sup>17–19</sup> see Table II. We find a small discrepancy with the Monte Carlo results of Ref. 24; see Table II. Note that the authors of Ref. 24 did not take into account a subleading correction with the exponent  $\omega'=1.67(11)$  (Ref. 44) analyzing their Monte Carlo data.

The accuracy that is reached now by lattice methods has clearly outpaced that of field theoretic methods. Furthermore, comparing with the numbers that are summarized in Table I, we notice that most of the results for  $\eta$  and  $\omega$  obtained from the perturbative expansion in three dimensions fixed are at odds with ours while those of Refs. 11 and 13 are in reasonable agreement. Note that, as discussed by Nickel,<sup>13</sup> the subleading correction exponent  $\omega'=1.67(11)$  (Ref. 44) also plays a crucial role in the analysis of the perturbative series in three dimensions fixed. Therefore, it would be highly desirable to get an independent confirmation of this result.

Using Monte Carlo simulations, the error of the estimates of the critical exponents can be further reduced just by spending more CPU time. To this end one has to increase the statistics as well as enlarge the size of the lattices that are simulated. Keeping the statistical error and the systematical one proportional, the effort increases as  $\text{error}^{-2-(3+z)/\omega'}$  with a decreasing error, where the first factor  $\text{error}^{-2}$  is related to the increased statistics and the second to the larger linear lattice size  $L$  that is needed to reduce the systematical error. Here we assume that the systematical error is proportional to  $L^{-\omega'}$ ,

since, as we have shown here, leading corrections can be eliminated. The effort at a fixed statistical accuracy behaves as  $L^{d+z}$ , where  $d=3$  is the dimension of the system and  $z$  is the critical dynamical exponent. In a recent study of a spin glass<sup>46</sup> about 1000 years of CPU time on one core of a CPU of similar performance as the one used here had been spent. This is about a factor of 30 more CPU time than we have spent here. One should notice however that this factor in

CPU time only would allow to reduce the errors of the critical exponents by a factor of about 2.3, where we have assumed  $\omega' \approx 1.6$  and  $z \approx 0.4$ ; see Eqs. (18) and (19).

#### ACKNOWLEDGMENT

This work was supported by the DFG under the Grant No. HA 3150/2-1.

\*martin.hasenbusch@physik.hu-berlin.de

- <sup>1</sup>K. G. Wilson and J. Kogut, *Phys. Rep.* **12**, 75 (1974).
- <sup>2</sup>M. E. Fisher, *Rev. Mod. Phys.* **46**, 597 (1974).
- <sup>3</sup>M. E. Fisher, *Rev. Mod. Phys.* **70**, 653 (1998).
- <sup>4</sup>A. Pelissetto and E. Vicari, *Phys. Rep.* **368**, 549 (2002).
- <sup>5</sup>J. V. Sengers and J. G. Shanks, *J. Stat. Phys.* **137**, 857 (2009).
- <sup>6</sup>M. Barmatz, I. Hahn, J. A. Lipa, and R. V. Duncan, *Rev. Mod. Phys.* **79**, 1 (2007).
- <sup>7</sup>A. Lytle and D. T. Jacobs, *J. Chem. Phys.* **120**, 5709 (2004).
- <sup>8</sup>K. G. Wilson and M. E. Fisher, *Phys. Rev. Lett.* **28**, 240 (1972).
- <sup>9</sup>G. Parisi, Cargese Lecture Notes, Columbia University preprint, 1973 (unpublished); *J. Stat. Phys.* **23**, 49 (1980).
- <sup>10</sup>K. G. Chetyrkin, S. G. Gorishny, S. A. Larin, and F. V. Tkachov, *Phys. Lett. B* **132**, 351 (1983); H. Kleinert, J. Neu, V. Schulte-Frohlinde, K. G. Chetyrkin, and S. A. Larin, *ibid.* **272**, 39 (1991); **319**, 545(E) (1993).
- <sup>11</sup>D. B. Murray and B. G. Nickel, revised estimates for critical exponents for the continuum  $n$ -vector model in three dimensions, unpublished Guelph University report, 1991. The coefficients of the loop expansion are reported, e.g., in Ref. 15. Numerical results for the critical exponents are reported in Table IV of Ref. 14.
- <sup>12</sup>R. Guida and J. Zinn-Justin, *J. Phys. A* **31**, 8103 (1998).
- <sup>13</sup>B. G. Nickel, *Physica A* **177**, 189 (1991).
- <sup>14</sup>H. Kleinert, *Phys. Rev. D* **60**, 085001 (1999).
- <sup>15</sup>F. Jasch and H. Kleinert, *J. Math. Phys.* **42**, 52 (2001).
- <sup>16</sup>A. A. Pogorelov and I. M. Suslov, *J. Exp. Theor. Phys.* **106**, 1118 (2008).
- <sup>17</sup>M. Campostrini, A. Pelissetto, P. Rossi, and E. Vicari, *Phys. Rev. E* **65**, 066127 (2002).
- <sup>18</sup>P. Butera and M. Comi, *Phys. Rev. B* **65**, 144431 (2002).
- <sup>19</sup>P. Butera and M. Comi, *Phys. Rev. B* **72**, 014442 (2005).
- <sup>20</sup>H. Ballesteros, L. Fernández, V. Martín-Mayor, G. Parisi, and J. Ruiz-Lorenzo, *J. Phys. A* **32**, 1 (1999).
- <sup>21</sup>M. Hasenbusch, K. Pinn, and S. Vinti, *Phys. Rev. B* **59**, 11471 (1999).
- <sup>22</sup>M. Hasenbusch, *J. Phys. A* **32**, 4851 (1999).
- <sup>23</sup>H. W. J. Blöte, L. N. Shchur, and A. L. Talapov, *Int. J. Mod. Phys. C* **10**, 1137 (1999).
- <sup>24</sup>Y. Deng and H. W. J. Blöte, *Phys. Rev. E* **68**, 036125 (2003).
- <sup>25</sup>K. Binder, *Z. Phys. B: Condens. Matter* **43**, 119 (1981).
- <sup>26</sup>M. N. Barber in *Phase Transitions and Critical Phenomena*, edited by C. Domb and J. L. Lebowitz (Academic, New York, 1983), Vol. 8.
- <sup>27</sup>*Finite Size Scaling and Numerical Simulation of Statistical Systems*, edited by V. Privman (World Scientific, Singapore, 1990).
- <sup>28</sup>M. Hasenbusch, F. Parisen Toldin, A. Pelissetto, and E. Vicari, *J. Stat. Mech.: Theory Exp.* (2007) P02016.
- <sup>29</sup>F. Benitez, J.-P. Blaizot, H. Chaté, B. Delamotte, R. Méndez-Galain, and N. Wschebor, *Phys. Rev. E* **80**, 030103(R) (2009).
- <sup>30</sup>M. Astorino, F. Canfora, and G. Giribet, *Phys. Lett. B* **671**, 291 (2009).
- <sup>31</sup>M. Deserno, *Phys. Rev. E* **56**, 5204 (1997).
- <sup>32</sup>J. R. Heringa and H. W. J. Blöte, *Phys. Rev. E* **57**, 4976 (1998).
- <sup>33</sup>Y. Deng and H. W. J. Blöte, *Phys. Rev. E* **70**, 046111 (2004).
- <sup>34</sup>M. Hasenbusch, *Int. J. Mod. Phys. C* **12**, 911 (2001).
- <sup>35</sup>H. W. J. Blöte, E. Luijten, and J. R. Heringa, *J. Phys. A* **28**, 6289 (1995).
- <sup>36</sup>M. Hasenbusch, *Physica A* **197**, 423 (1993).
- <sup>37</sup>M. Campostrini, M. Hasenbusch, A. Pelissetto, and E. Vicari, *Phys. Rev. B* **74**, 144506 (2006).
- <sup>38</sup>R. C. Brower and P. Tamayo, *Phys. Rev. Lett.* **62**, 1087 (1989).
- <sup>39</sup>J. A. Plascak, A. M. Ferrenberg, and D. P. Landau, *Phys. Rev. E* **65**, 066702 (2002).
- <sup>40</sup>See, e.g., S. Wansleben, J. B. Zabolitzky, and C. Kalle, *J. Stat. Phys.* **37**, 271 (1984); G. Bhanot, D. Duke, and R. Salvador, *Phys. Rev. B* **33**, 7841 (1986).
- <sup>41</sup>U. Wolff, *Phys. Rev. Lett.* **62**, 361 (1989).
- <sup>42</sup>M. Saito and M. Matsumoto, in *Monte Carlo and Quasi-Monte Carlo Methods 2006*, edited by A. Keller, S. Heinrich, and H. Niederreiter (Springer, Berlin, 2008); M. Saito, M.S. thesis, Hiroshima University, 2007; the source code of the program is provided at <http://www.math.sci.hiroshima-u.ac.jp/~m-mat/MT/SFMT/index.html>
- <sup>43</sup>F. Panneton, P. L'Ecuyer, and M. Matsumoto, *ACM Trans. Math. Softw.* **32**, 1 (2006); the source code of the program is provided at <http://www.iro.umontreal.ca/~panneton/WELLRNG.html>
- <sup>44</sup>K. E. Newman and E. K. Riedel, *Phys. Rev. B* **30**, 6615 (1984).
- <sup>45</sup>M. Campostrini, A. Pelissetto, P. Rossi, and E. Vicari, *Phys. Rev. E* **57**, 184 (1998).
- <sup>46</sup>L. A. Fernandez, V. Martín-Mayor, S. Perez-Gaviro, A. Tarancon, and A. P. Young, *Phys. Rev. B* **80**, 024422 (2009).